THE AMERICAN JOURNAL OF PATHOLOGY

VOLUME XLIV JANUARY, 1964 NUMBER 1

A DESCRIPTION OF ECHO-9 VIRUS INFECTION IN CULTURED CELLS

I. THE CYTOPATHIC EFFECT

GABRIEL C. GODMAN, M.D.; RICHARD A. RIFKIND, M.D.*; CALDERON HOWE, M.D., AND HARRY M. ROSE, M.D.

From the Department of Microbiology, College of Physicians and Surgeons, Columbia University, New York, N.Y.

The consequences of infection of cells in tissue culture with certain small RNA-viruses are now among the best understood of infectious cytocidal processes, and an abundant literature on the cycle of viral development and release and certain of the cytopathic effects, especially of poliovirus, has accumulated. Extension of our earlier observations with the electron microscope [1] on the development of ECHO virus serotype 9 (enterovirus 40) by other cytologic and cytochemical means has provided additional insights into the morphogenesis and chemical features of the cellular changes. An opportunity is thus afforded to present a more complete picture of the events that follow upon ECHO virus infection in which certain visible alterations of the cell can be correlated with and occasionally explained by changes in chemical composition or synthetic function.

Although the intracellular events whereby one or a few particles of this agent bring about dramatic and ultimately lethal effects are by no means all resolved, certain generalizations are beginning to emerge. These seem in outline, if not in detail, to be valid for all the enteroviruses and, at least, some members of the Columbia SK group. The ensuing account

These studies were supported by the Jane Coffin Childs Fund for Medical Research, by The National Foundation, and by the Office of the Surgeon General, Department of the Army, under the auspices of the Commission on Influenza, Armed Forces Epidemiological Board.

Accepted for publication, August 5, 1963.

* Present address: Department of Medicine, College of Physicians and Surgeons, Columbia University, New York 32, N.Y.

is intended as a cytologic description relating different aspects of these changes as they appear after ECHO-9 infection.

Material and Methods

Rhesus monkey epithelial (MK) cells, obtained from trypsinized normal kidney tissue were propagated in Melnick's serum-lactalbumin hydrolysate medium [2] from 5 to 10 days, until a confluent cell sheet developed. The cells were again trypsinized, washed and suspended in fresh medium, and aliquots were dispensed either into Leighton tubes in which a cover slip had been placed or into 25 ml. plaque bottles. After growth, the cell sheets were washed with Earle's balanced salt solution and in most instances were inoculated with 5×10^5 tissue culture infective doses (TCID) of type 9 ECHO virus (Hill strain). In other experiments in which a maximal number of infected cells was desired ("one-step" growth curve), tubes or bottles were inoculated with 0.2 ml. of an estimated 4.0 to 4.6×10^6 plaque forming units (PFU) per ml. dose of virus, representing a final multiplicity of approximately 30 to 40. Cultures were occasionally checked for hemadsorption agents [3] and demonstrable simian viruses.

Cells destined for electron microscopy were scraped from the flasks into balanced salt solution, centrifuged into pellets which were fixed in buffered osmium tetroxide, dehydrated in graded dilutions of ethyl alcohol, embedded in methacrylate and sectioned in the ultramicrotome. Most mounted sections were stained with lead hydroxide.[4]

For supravital observations with the phase microscope, cells were grown on cover slips which were either enclosed in a Sykes-Moore chamber or inverted onto glass slides and sealed with silicone grease, and maintained at about 37° C. in a microscope stage incubator. Supravital staining was carried out by mounting the cell sheet on a slide whose surface had been prepared by complete evaporation of 0.5 per cent alcoholic solutions of either Janus green or neutral red (National Aniline).[5]

For light microscopy, cell sheets on cover slips were usually prepared by quenching at about −170° and substitution [6] in one of the following at about −50° C.: methanol; anhydrous charcoal-treated acetone; Carnoy's fluid; methanol saturated with mercuric chloride or with picric acid. Cover slips were otherwise fixed in anhydrous methanol at 0° C., or in either 10 per cent phosphate-buffered formalin, pH 7.0, or in 1 per cent calcium chloride in 10 per cent neutralized formalin, at 0° C.

As an oversight stain, aqueous azure A or B followed by brief differentiation and counterstain in alcoholic eosin Y was satisfactory. Mitochondria were stained, after fixation in cold Helly's fluid, with Regaud's iron hematoxylin.

Observations

The Infected Population

At low doses (less than 5 PFU per cell or 2.0 to 5.0×10^5 TCID), chosen because the slower progression of the morbid changes in the cells facilitated close study, a response of more than 45 per cent of adherent, pathologically altered cells was rarely achieved by 18 hours. Between 18 and 22 hours, at the height of the effect, the cell sheet was punctuated by numerous demarcated dense foci with a tendency to confluence; these subsequently became the definitive plaques. The foci were round, measured from 0.1 to 0.8 mm. or more, and consisted of central cores of retracted, separated, heavily staining cells surrounded by concentric

whorl-like formations of elongated diseased cells. Small collections of altered cells seen in earlier phases constituted the centers of the foci. The latter developed by centrifugal spread, as suggested by the more advanced state of the central lesions and the earlier changes in the more peripheral cells.

Rate of Infection

Specimens taken at intervals after inoculation of virus established the sequence of pathologic changes characteristic of early, intermediate, late and terminal stages. Relative counts of these at each time point indicated that after inoculums of less than 5 PFU per cell, an over-all two-step cycle (i.e., one cycle of re-infection) was taking place. After low doses, early stages were present in greatest number between 6 and 8 hours, declined and reappeared at 18 to 22 hours; intermediate and later stages predominated between 12 and 18 hours, decreased and were again very numerous only at 20 to 24 hours (50 to 70 per cent of adherent cells). At 14 hours only about 35 per cent of cells showed signs of infection, and even after 24 hours only about 50 per cent of adherent cells were infected. Late stages tended to accumulate and to remain relatively stationary for long periods. At high viral multiplicities (40 or more PFU per cell or 1.2×10^6 TCID) there was a higher initial rate of infection (about 30 per cent at 8 hours, compared with 15 to 20 per cent after low doses) as judged by cytopathic effect, and a one-step cycle. Nevertheless, not more than 70 to 80 per cent of cells were visibly infected at 20 hours. However, in cells which became infected, the alterations progressed more rapidly, beginning at about 4 hours, becoming florid at 6 to 8 hours and far advanced by 10. The continuous cell changes after infection occurred only roughly parasynchronously after large doses of virus, and even less so after smaller doses when variation from cell to cell was greater.

Continuous observation of the same field with the phase microscope showed cells at differing stages in infection, and the changes proceeding at differing rates after inoculation of ECHO-9 virus. The gradually rising index of infection during the first 8 to 10 hours even after infection with high multiplicities of virus, and the persistence of some early and beginning midstages at 8 to 12 hours after inoculation with less than 5 PFU per cell, probably reflected a lag in the progress of visible cell changes rather than a new cycle of infection (second-step growth curve), which only began after 16 hours.

The rate of infection and the relative incidence of each stage of infection are tabulated in Table I. If a steady state could be assumed, the incidence of the different stages at successive intervals might be used as a basis for calculating mean time of sojourn (transit time) for each, but

TABLE I

PROPORTION OF CELLS WITH PATHOLOGIC CHANGES AFTER INOCULATION OF MONOLAYERS OF MK CELLS WITH HIGH AND LOW DOSES OF ECHO-9 VIRUS

Hours after infection	High dose: 1.2×10^6 TCID *							Low dose: 2.0×10^5 TCID						
	All stages % of tot.	Early		Mid		Late		All stages % of tot.	Early		Mid		Late	
		% of tot.	% of inf.	% of tot.	% of inf.	% of tot.	% of inf.		% of tot.	% of inf.	% of tot.	% of inf.	% of tot.	% of inf.
3	6.3	6.3	100	0	0	0	0							
4	13.1	13.1	100	0	0	0	0	3.0	3.0	100	0	0	0	0
5	10.7	4.8	45.0	5.9	55.0	0	0	13.8	13.8	100	0	0	0	0
6	32.9	17.2	52.1	15.7	47.9	0	0	13.0	8.5	65.8	4.5	33.9	0	0
7	29.8	6.4	21.4	23.4	78.6	0	0	18.7	8.5	45.5	10.2	54.4	0	0
10	73.6	6.1	8.0	47.8	63.0	21.4	29.0	29.4	13.6	42.8	15.2	51.4	1.6	5.7
11	47.4	2.4	6.5	25.1	53.9	20.4	46.5							
12	59.4	1.8	3.0	24.3	40.9	33.3	56.0	47.0	4.2	8.9	29.4	62.5	13.4	28.6
15								38.5	1.6	4.3	14.0	36.2	22.9	59.4
16								46.9	2.3	4.8	17.4	37.1	27.2	58.0
20	52.48	1.6	3.1	4.9	9.3	45.9	87.5	60.0	4.2	7.2	23.9	39.7	31.8	53.0
22								55.7	8.1	14.7	13.1	23.5	35.2	63.2
24								60.1	8.2	14.0	11.4	20.2	42.9	68.5

* Tissue culture infective doses.

Key: tot. = total. inf. = infected.

because of variability from cell to cell such estimations would only be approximate.

Mitotic Index

Cells in mitosis averaged 3.36 per thousand (range, 0 to 7.5) in control populations of monkey kidney cells on maintenance medium. In infected cultures, the over-all index of mitosis declined to an average 0.8 per thousand; the average number of mitotic figures remaining in intact (i.e., normal-appearing) cells was also lower than in the controls (average, 1.9 per thousand; range, 0 to 2.9) up to 24 hours. A rough inverse correlation was found between the number of mitotic figures in any field and the density of adherent cells in the field.

CELLULAR CHANGES AND THEIR PROGRESSION

Monkey Kidney Cells

Sheets used for infection were monolayers of partly contiguous cells which, unless constrained by crowding, grew as very extenuated elements flattened against the vessel floor. With transmitted light, the cell outline usually was indistinct as a result of attenuation of the marginal fringe; it could be revealed in phase contrast as an active ruffled velum. The nuclei were flattened or lenticulate, round, and of variable size. The average product of major and minor diameters was 103.5 μ and range 35.5 to 212 μ, a parameter related to degree of ploidy, most often with a single large diffuse and heterogeneous nucleolus. With azure-eosin the nuclear contents were stained pinkish, the nucleolus purplish and the general cytoplasm diffusely violet. The numerous mitochondria in these cells were all filamentous and disseminated throughout all parts of the cytoplasm (Fig. 1).

Four stages could be distinguished in the continuous sequence of alterations occurring after infection:

Early Stage

In fixed preparations, the earliest discernible changes within the cell were tinctorial. A zone of increased basophilia developed at the nuclear membrane and the immediately adjacent cytoplasm, usually in one sector. Accompanying this, small floccules, staining faintly blue-green with azure or azure-eosin, made their appearance in the nucleus. The nucleolus subsequently became more condensed and deeply colored (Fig. 11 in Part II [7]). The cell outlines now appeared with better definition and exhibited more irregular lines. A spatial separation of the affected cell from its neighbors, the result of retraction, was quite evident in both living and stained preparations (Fig. 2). In the living state, the cell surface was

more active, and some sectors showed an enhancement of phase density. The mitochondria tended to become nodose and to gravitate toward the center of the cell where perinuclear granules, refractile in the living cell (Figs. 3 and 4) and chromophobic after azure-eosin staining, began to accumulate. The early, more diffuse perinuclear basophilia was transitory, but more compact circumscribed masses of basophilic material remained associated with the nuclear membrane.

Intermediate or Mid Stage

In the mid stage the dendritic, more refractile cell (Fig. 5) typically exhibited a peripheral basophilic rim, an eccentrically placed shrunken distorted nucleus and a large round central or juxtanuclear mass which remained unstained with azure-eosin in fixed preparations (Fig. 13). This form evolved by continued retraction of the cell and a marked symmetrical expansion of the juxtanuclear mass content. Occupation of the cell center by growth of this large circumscribed mass displaced basophilic elements of the cytoplasm to the cell periphery, where they formed a cortical mantle or rim. The nucleus was also, probably passively, forced to the periphery of the firm central mass, against which it was molded. It lay like a cap or crescent between the round chromophobic centricellular mass and the now basophilic cell periphery.

Nucleus. The nucleus underwent profound structural and tinctorial alterations: the floccules of the early stage which stained blue-green with azure coalesced into strands deposited against the inner aspect of its membrane. The nucleus was sometimes elongated in one axis, as though stretched, drawing out parallel plications of its membrane (Fig. 11). The plications later became less regular, and as the nucleus collapsed, as though from a loss of turgor, the membrane crumpled. Its outpocketed ridges (gyri) and the infolded intervening declivities (sulci) were apparent in living cells (Figs. 4 to 8) and in stained whole mounts (Fig. 13). Nuclear collapse and shrinkage occupied a relatively short time (about 20 to 30 minutes) in living cells. In thin sections the ridges were found to be packed with condensed, very finely granular or thready chromatin filaments which stained blue-green with azure.

Within the deep intervening incisures or infoldings between the crests always just external to the outer nuclear membrane, closely compacted masses of hundreds of ribosomal granules, each 15 to 18 mμ in diameter were frequently found. Viewed in whole mounts, the shrunken wrinkled nucleus was beset by many round or linear masses staining violet-purple with azure or azure-eosin (in contrast to the blue-green stain of the condensed chromatin) and which lay within the bays between the nuclear ridges (Fig. 12, and Figs. 1 to 5 in Part II [7]). They corresponded to the

aggregations of ribosomes embraced by the nuclear outpocketings, as seen with the electron microscope (Fig. 12, and Figs. 1 and 23 in Part II[7]). The convoluted nuclear membrane itself was unaltered save for a well-marked expansion, usually focal, of the space separating inner and outer membranes. Into this space small ribosome-containing invaginations of outer nuclear membrane, and nuclear herniations invested with inner membrane might protrude as fingers (Fig. 12, and Fig. 1 in Part II[7]). Fenestrations or pores were numerous. On the nuclear side they were continuous and showed prominent rarefactions in the dense chromatin; the communicating cytoplasm immediately opposite the fenestration was also less dense. The nucleolus persisted as a smaller, compact, deeply staining structure throughout the mid stage, usually in the less dense central part of the distorted nucleus. By electron microscopy it was most often represented by aggregations of dense 16 to 20 mμ granules with electron-transparent gaps between them (Fig. 12) and occasionally as a random collection (Fig. 22). Scattered seemingly at random, dense ribosome-like interchromatinic granules appeared among the condensed chromatin filaments as well as in the more rarefied nuclear center. In the latter, other bodies of unknown nature could also be perceived (Figs. 22 and 23). These measured 300 to 500 mμ, were moderately adielectronic (electron scattering), and usually finely granular or finely filamentous. Less often they exhibited patterns showing a regular linear or crystalline order.

Chromophobic Centricellular Mass. The pale material of the centricellular mass usually began to accumulate in the Golgi zone of the juxtanuclear region very soon after the first appearance of enhanced perinuclear basophilia. Its continued exclusive growth appeared to have been responsible for forcing the other cellular elements peripherally. At its greatest development it was seen in the living cell as a heterogeneous structure of high refractility but low density, containing small, more refractive granules and globules (Figs. 4, 5, 10 and 11). Filamentous or rodlike mitochondria were found only in its peripheral zone. In the living cell, no (Brownian) movement was discernible. If the infected cell was compressed, the mass resisted deformity more than other cell structures, and it persisted as an entity after cytolysis or mechanical disruption. After the administration of dilute neutral red to infected cultures, the dye was found concentrated as granules in scattered loci within and especially at the fringe of this area (Fig. 10). In frozen-substituted or formalin-fixed monolayers, its components resisted staining with both acid and basic dyes from pH 2.6 to pH 7.0, but after fixation in Helly's fluid, it was moderately acidophilic.

By electron microscopy the centricellular mass appeared to consist of

various sized (25 to 1,000 mμ) congeries of smooth-walled vesicles and their membranous derivatives (Figs. 9, 12, 22 and 23 in Part II [7]). Most were either spheroidal or elongated profiles bounded by single smooth membranes. Invaginations leading to more complex pictures were evident, the most common being represented by two concentric profiles of smooth membrane 20 to 40 mμ apart, the inner lamella circumscribing a plug of ground cytoplasm. However, vesicles surrounded by multiple wavy concentric membranes were frequent, and appeared to be related to the tighter concentric myelin-like figures (spherulites) often found in this region (Figs. 22 and 23 in Part II [7]). Small fat droplets were also present. Most of the larger singly lamellated vesicles appeared to be empty, but many, especially the small ones, contained remnants of slight to moderately adielectronic material, and large (20 to 30 mμ) dense granules. Where membranous components were not in apposition, they were separated by a very finely granular or reticular ground cytoplasm.

The Basophilic Material. With the pre-emption of the cell center by a chromophobic mass, the basophilic components were displaced and compressed. The diffuse basophilia was represented electron microscopically by disseminated free ribosomes lying singly or in very small clusters, and by occasional cisterns of the rough-surfaced endoplasmic reticulum. The channels of the latter were often widely dilated and contained material of moderate electron density. Most of the basophilic material of the cell, however, was gathered into clumps and masses represented by large aggregations of ribosomes. These came to lie not only in the nuclear crevices but also throughout the cortex of the cell (Figs. 12 and 13). The mantle zone of the cell then appeared mottled or "tigered" as the result of numerous metachromatic, azurophilic granules and masses measuring 1 to 10 μ or more in size. These were most numerous near the nucleus. Accurate estimation of the numbers of ribosomes comprising a large aggregate would be difficult because of variations in aggregate size and density. However, the major aggregates appeared to be conglomerates of smaller clusters, each consisting of some 20 to 40 ribosomes as counted in sections about 60 to 80 mμ thick (Fig. 12). These smaller clusters were elongated in shape, usually curved and sometimes serpentine. The ribosomes composing the small clusters were usually arrayed in short linear or filar series, and in rare instances the rows were oriented upon a thin, delicate line (15 to 20 Å) continuous from particle to particle (inset, Fig. 12). Moreover, the dense ribosomes in small clusters were embedded in an amorphous, diffuse, slightly adielectronic material, denser than the lighter regions intervening between the clusters.

The Mitochondria. By midstage, filamentous and stubby rod-like mitochondria had congregated in great numbers about the juxtanuclear

mass which they closely surrounded and whose periphery they penetrated (Figs. 10 and 25, Part II [7]). The main mass of mitochondria then formed a discontinuous wreath between the juxtanuclear mass of membranes and vesicles and the basophilic cell cortex; the nucleus was also beset by these organelles. They were remarkable in stained preparations for their excellent preservation after alcoholic fixation, and for their apparently enhanced basophilia (Fig. 13). As early as the intermediate stage, mitochondrial swelling was especially a feature in some of those which had penetrated into the juxtanuclear mass; appearances suggestive of mitochondrial disintegration could be seen (Figs. 23 and 26, Part II [7]). These changes became more frequent as the cytopathic effect progressed.

The Virus. Ordered linear aggregates of viral particles were found throughout the cytoplasm. These were mostly at the edges of the juxtanuclear collection of vesicles, although some occurred more peripherally in the basophilic region or within the central mass of vesicles (Figs. 12, 22 and 23 and Figs. 18 and 23 in Part II [7]). The structure of these composite paracrystalline arrays has been described previously.[1] They consisted of a series of parallel linear files composed of spheroidal particles, (22 to 24 mμ), closely stacked, and separated by filaments, 2 to 5 mμ in diameter, which frayed out into tassels meshing with unordered arrays of similar cytoplasmic fibrils. Transverse sections showed the filaments to be arranged in hexagonal order about each row of viral particles; each row of particles was surrounded by a hexagon of 6 adjacent rows of viral particles.

In continuity with these organized formations of virus, small masses of a very finely granular and filamentous material were occasionally encountered. They were small and had not been identified with the light microscope. Because of their intimate spatial relationship to the viral arrays, they were believed to represent sites within which viral particles were assembled and aligned upon filamentous lattices.[1]

The viral particles were not only larger but were stained more intensely with lead or uranyl salts than ribosomes. Especially in the later stages, unorganized collections of such particles were encountered in both the cortex and the center of the cell.

Shedding

Increased activity of the cell surface was manifest in the early stages of infection, and discharge of cell materials at the surface was well-marked by mid stage. The mid stage of the cellular lesion was followed by a period of greatly accelerated decortication (ecdysis) of the basophilic outer mantle of cytoplasm. This remarkable process, which could be followed in the living cell with the phase microscope (Figs. 3 to 8, 11 and

19) was brought about in two ways. Usually there was a protrusion of many bulbous or longer lanceolate cytoplasmic processes from all parts of the cell surface, the latter being cell attachments elongated by retraction of the cell body. These extensions carried with them globules of cortical cytoplasm and became detached from the affected cell by prolongation and attenuation of their stalks (leaving behind retracted scrolls of cytoplasm). Included within most of the separated fragments were basophilic masses, which were dense aggregates or looser masses of ribosomes (Figs. 3 to 8 and 14 to 17).

Another mechanism which served to partition and ultimately to separate the superficial cytoplasm began early in the middle phase with the formation of vacuoles and cysts. Most of these first became apparent in and near the chromophobic centricellular mass, but some appeared to originate in the basophilic cortex itself. They developed by dilatation and coalescence, usually of some of the smooth-walled vesicles, but occasionally also by swelling of remnants of rough-surfaced endoplasmic reticulum. These filled with watery content of low density, became increasingly distended, fused, and tended to form cysts. They migrated to the cell surface, where they might burst, lifting off layers of overlying cortical cytoplasm in the process (Figs. 3 to 8 and 18 to 21). Otherwise, retained in the cortex, they infiltrated the cytoplasm in such numbers and became so dilated that a reticulated or spongy mesh was formed in which the vacuoles were separated by a net or basketwork of cytoplasm (Fig. 20). In either case, the whole cell cortex with its basophilic material was ultimately sloughed. Among the formed elements discernible within or upon the cytoplasmic protrusions were, besides the ribosomal masses (Figs. 14 and 16), occasional vesicles and small collections of viral particles (Fig. 14).

Terminal Stage

Until the occurrence of rapid cortical sloughing, the continuity of the distorted nuclear membrane was usually preserved. It had shrunk to about a quarter of its original size (mean product of major and minor axes, 23.0 μ; range, 15 to 70 μ). Further collapse and condensation of chromatin resulted in extreme convolution and plication and a formation of thin lamellas packed with chromatin (Fig. 1 in Part II[7]). The nucleolus occasionally persisted as a recognizable entity within the crumpled sac of the pyknotic nucleus (Figs. 22 and 23), but more often it disappeared. Karyorrhexis might then occur with the dispersion of nuclear lobules or fragments in the adjacent cytoplasm. Azurophilic metachromatic masses remained associated with both the detaching fragments and the main body of the disintegrating nucleus. Karyorrhexis

did not occur in all cells late in infection, and on occasion it began as early as midphase. Ultimately, when most of the basophilic cortex had been shed, there remained a nucleated cell remnant of regular outline with little or no cytoplasmic basophilia (Fig. 21). The cytoplasmic remnant, at first somewhat chromophobic, became increasingly acidophilic as karyorrhexis and disintegration proceeded.

Discussion

Viral Growth Cycle and Cytopathic Effects

It is well known that all of the enteroviruses bring about cytopathologic changes of a smiliar kind [8–10] and that the cellular lesions provoked in tissue culture by other small RNA viruses like EMC and Mengo of the Columbia SK group are analogous.[11,12] Their apparent similarities have led Andrewes and colleagues [13] to group a number of these small RNA viruses under the name "nanivirus" (dwarf virus).

Not all the cells succumb to high multiplicities even of poliovirus, for which a one-step growth curve with "universal" infection has frequently been assumed.[14,15] With ECHO-9, after high multiplicities, not more than about 70 to 80 per cent of the cell population ultimately exhibited typical cytopathic changes. At low doses the number of infective centers was limited by dilution and scattered distribution of viral particles. At very high multiplicities, however, in which homogeneous distribution is assumed, the apparent resistance of some fraction of the cell population to cytocidal consequences must be related to factors other than lack of contact between cell and virus. Among these might be altered surface properties and failure of adsorption,[16] inability of certain cells to release infectious RNA from the viral shell after viral entry,[17,18] interference phenomena, phase in mitotic cycle, or to yet other states.[19–21] Of interest was the asynchrony with which the successive stages leading to shedding and cell death proceeded among individual members of a population of cells simultaneously inoculated. This variability, which has been emphasized [14,22,23] for poliovirus in HeLa cells, has also been noted in L cells infected with Mengo virus.[11] When, after ECHO-9 infection, the changes characteristic of intermediate stages began, numbers of cells in all except the latest stages of infection could be found, although at any given time the majority of cells was approximately in the same phase. A phenomenon probably related to this is the apparent foreshortening in time of the lethal cell changes and the earlier appearance of cytopathic effects as the viral multiplicity is increased.[9,14,15,23,24] This suggests that the greater the amount of infective RNA released into the cell, the more rapid the changes in the cycle of viral multiplication. At high multiplicities of ECHO-9 the schedule of changes was only slightly slower than reported

for the polio virus.[14,23,24] Thus asynchrony in onset and progression of the morbid process may reflect accidental differences in the number of viral particles absorbed or capable of being dismantled by individual cells. However, differences from cell to cell in the duration of each phase may also be due to physiologic variations among cells, as suggested by the somewhat different viral yields and growth curves obtained from different single cells infected with the same dose of poliovirus.[24] Such variations from cell to cell in respect to the rate of viral synthesis might possibly be related to initial differences in content of available ribosomes, degree of polyploidy, and phase of mitotic cycle at the time of infection.

At the time of inoculation most of the monkey kidney cultures used in the present study were not growing rapidly. Since infected cells are apparently no longer capable either of mitotic division or of premitotic DNA synthesis, it was not unexpected that the over-all mitotic rate should have declined after infection.[14] It is of interest, however, that the index calculated for the remaining cells without evidences of infection should also have fallen. Possibly some among these were lagging in very early (eclipsed) phases of infection, but the explanation is not obvious.

Although transit times were not calculated from the data shown in Table I, for a given dose it is possible, by continuous observation of living infected cells, to assign a relative duration with respect to the time required for the whole sequence in any stage. Thus, at moderately high multiplicities the early events were rapid (about 1/6 of the cycle); nuclear collapse, once it started, was most rapid (about 1/12 of the cycle or less). Although some cortical shedding began early and continued, massive decortication occurred chiefly within 1 to 2 hours (about 1/8 to 1/6 of the cycle). The midperiod, before accelerated shedding, and the late stages were relatively longer pauses.

The Sequence of Structural Changes

The earliest discernible change after poliovirus infection has been variously described,[8,14,15,25-27] perhaps because a number of rearrangements occur simultaneously. Although morphologically more subtle, these early events are of the greatest importance in the synthesis of viral materials. In ECHO-9 infection, the early visible changes were: (a) alterations of the cell surface, leading to increased refractivity, increased movement of the ectoplasmic velum, retraction of the cell margins and loss of contact with neighboring cells; and (b) the accumulation of diffuse, phase-dense, basophilic material about the nuclear membrane. Very rapidly thereafter, increased numbers of highly refractile lipid-containing granules appeared in the cytoplasm in the juxtanuclear centrospheric or Golgi zone, at the same time that flocculation of chromatin

within the nucleus became evident. There then ensued a concentration of the basophilic material. By this time synthesis of viral materials was under way, even before any marked nuclear shrinkage had taken place. The tendency of the cytoplasmic basophilic material to form granules or blocs has been noted by some observers in poliovirus infection [9,15,22]; it was an outstanding feature of ECHO-9 infection in MK cells in which the blocs were composed of structured aggregations of ribosomes. The significance of the agglutination of ribosomes will be further considered in the discussion of RNA.

Subsequent changes leading to the mid phase of infection were merely continuations or consequences of these earlier processes. Nuclear collapse was accompanied by margination, i.e., precipitation of chromatin against the nuclear membrane, loss of nuclear "sap," and nucleolar condensation, alterations interpretable as a kind of pyknosis.

The most obvious feature in the mid stage was the central mass, to which attention has been drawn by investigators of poliovirus infection [8,15,25–28] and ECHO virus infection [1,8,29] (Figs. 4, 10, 12 and 23 in Part II [7]) .The Golgi apparatus, in whose territory this mass developed, became lost as a recognizable entity in its midst; its part in the new formation of these membranes deserves study. None of the latter have the pyrophosphatases invariably associated with the lamellar components of the Golgi apparatus, although neutral red continued to be transported and concentrated in that vicinity (Fig. 10). The rigidity and compactness of this mass has been emphasized in the present description and by observers of polio infection.[25–27] Since other structures cannot find receptivity within it, they must be displaced by its growth.

The peripheralization of basophilic (i.e., ribosomal) material insured the discharge of most of it from the cell during the process of decortication which began early in the mid stage. That shedding might be related to maximal release of polio virus from the cell was proposed by Barski, Robineaux and Endo [25] and later shown in studies correlating cytologic features with the virus titer.[15,22,24,30,31] Release occurs well after virus maturation, and is an unrelated process.[22,23,30] It may perhaps be regarded as a morbid exaggeration of a process of exocytosis of bodies foreign to the cytoplasm.

Summary

After infection of cultured rhesus monkey kidney cells with high doses of ECHO-9 virus, not more than about 75 to 80 per cent of the cell population exhibited pathologic changes. Although a one-step growth cycle ensued, the series of characteristic changes proceeded asynchronously in different cells, a phenomenon possibly related to the phase of the cell

cycle at the time of infection. The mitotic rate of the uninfected cells in the culture was depressed. The infected cell underwent a sequence of changes beginning at about 4 hours, at which time retraction of the cell and condensation of chromatin and nucleoli were seen. These were followed by nuclear collapse and convolution of its membrane. At the same time the cell center became occupied by a firm mass consisting of a congeries of smooth-surfaced vesicles and membranes, surrounded by a wreath of altered mitochondria. The basophilic material of the cytoplasm consisted chiefly of ordered aggregations of ribosomes imbricated in the sulci of the convoluted nucleus or displaced to the periphery of the cell. By means of vacuolation and detachment of cell processes at the surface, most of the peripherally located ribonucleoprotein masses were discharged into the medium together with some viral particles. Viral particles were organized and ordered into crystalline arrays at well-defined assembly sites.

References

1. Rifkind, R. A.; Godman, G. C.; Howe, C.; Morgan, C., and Rose, H. M. Structure and development of viruses as observed in the electron microscope. VI. ECHO virus, type 9. *J. Exper. Med.*, 1961,114, 1–12.
2. Melnick, J. Tissue culture techniques and their application to original isolation, growth and assay of poliomyelitis and orphan viruses. *Ann. New York Acad. Sc.*, 1955, 61, 754–773.
3. Vogel, J., and Shelokov, A. Adsorption-hemagglutination test for influenza virus in monkey kidney tissue culture. *Science*, 1957, 126, 358–359.
4. Dalton, A. J., and Zeigel, R. F. A simplified method of staining thin sections of biological material with lead hydroxide for electron microscopy. *J. Biophys. & Biochem. Cytol*, 1960, 7, 409–410.
5. The Microtomists Vade Mecum (Bolles-Lee). A Handbook of Methods of Animal and Plant Microscopic Anatomy. Gatenby, J. B., and Beams, H. W. (eds.). The Blakiston Co., Philadelphia, 1950, ed. 11, 753 pp.
6. Deitch, A. D., and Godman, G. C. The application of a freezing-substitution method of fixation to tissue culture preparations. *Anat. Rec.*, 1955, 123, 1–17.
7. Godman, G. C.; Rifkind, R. A.; Page, A. B., and Rose, H. M. A description of ECHO-9 virus infection in cultured cells. II. Cytochemical observations. *Am. J. Path.*, 1964, 44. (To be published)
8. Bernkopf, H., and Rosin, A. Cytopathologic changes in tissue cultures of human amnionic cells infected with poliomyelitis, Coxsackie, and ECHO viruses. *Am. J. Path.*, 1957, 33, 1215–1227.
9. Shaver, D.; Barron, A. L., and Kurzon, D. T. Cytopathology of human enteric viruses in tissue culture. *Am. J. Path.*, 1958, 34, 943–964.
10. Walker, D. L. *In vitro* cell virus relationships resulting in cell death. *Ann. Rev. Microbiol.*, 1960, 14, 177–196.
11. Dales, S., and Franklin, R. M. A comparison of the changes in fine structure of L cells during single cycles of viral multiplication, following their infection with the viruses of Mengo and encephalomyocarditis. *J. Cell Biol.*, 1962, 14, 281–302.

12. HINZ, R. W.; BARSKI, G., and BERNHARD, W. K. An electron microscopic study of the development of the encephalomyocarditis (EMC) virus propagated *in vitro*. *Exper. Cell Res.*, 1962, 26, 571–586.

13. ANDREWES, C. H.; BURNET, F. M.; ENDERS, J. F.; GARD, S.; HIRST, G. K.; KAPLAN, M. M., and ZHDANOV, V. M. Taxonomy of viruses infecting vertebrates: present knowledge and ignorance. *Virology*, 1961, 15, 52–55.

14. DUNNEBACKE, T. H. Correlation of the stage of cytopathic change with the release of poliomyelitis virus. *Virology*, 1956, 2, 399–410.

15. REISSIG, M.; HOWES, D. W., and MELNICK, J. L. Sequence of morphological changes in epithelial cell cultures infected with poliovirus. *J. Exper. Med.*, 1956, 104, 289–304.

16. MCLAREN, L. C.; HOLLAND, J. J., and SYVERTON, J. T. Cellular factors associated with susceptibility and resistance to enteroviruses. Nat. Cancer Inst. Monograph No. 7. 1962, pp. 273–285.

17. DARNELL, J. E., JR., and SAWYER, T. K. The basis for variation in susceptibility to poliovirus in HeLa cells. *Virology*, 1960, 11, 665–675.

18. JOKLIK, W. K., and DARNELL, J. E., JR. The adsorption and early fate of purified poliovirus in HeLa cells. *Virology*, 1961, 13, 439–447.

19. SOLOVIEV, V. C., and SEMENOV, B. F. Influence sur la virulence et les caractères antigéniques du virus de la poliomyélite de type 1, de la culture prolongée *in vitro* sur cellules rénales de singe. *Ann. Inst. Pasteur*, 1961, 100, 805–811.

20. WEINSTEIN, L., and CHANG, T.-W. Effect of "sex" of tissue cultures on growth of encephalomyocarditis virus. *Proc. Soc. Exper. Biol. & Med.*, 1961, 108, 471–474.

21. MURPHY, W. H., and LANDAU, B. J. Clonal variation and interaction of cells with viruses. Nat. Cancer Inst. Monograph 7, 1962, pp. 249–271.

22. ACKERMANN, W. W.; RABSON, A., and KURTZ, H. Growth characteristics of poliomyelitis virus in HeLa cell cultures: lack of parallelism in cellular injury and virus increase. *J. Exper. Med.*, 1954, 100, 437–450.

23. HOWES, D. W. The growth cycle of poliovirus in cultured cells. III. The asynchronous response of HeLa cells multiply infected with type 1 poliovirus. *Virology*, 1959, 9, 110–126.

24. LWOFF, A.; DULBECCO, R.; VOGT, M., and LWOFF, M. Kinetics of the release of poliomyelitis virus from single cells. *Virology*, 1955, 1, 128–139.

25. BARSKI, G.; ROBINEAUX, R., and ENDO, M. Phase contrast cinematography of cellular lesion produced by poliomyelitis virus *in vitro*. *Proc. Soc. Exper. Biol. & Med.*, 1955, 88, 57–59.

26. KLÖNE, W. Untersuchungen zur Cytopathogenität des Poliomyelitis virus (Typ Leon). *Arch. ges. Virusforsch.*, 1955, 6, 36–44.

27. HARDING, C. V.; HARDING, D.; MCLIMANS, W. F., and RAKE, G. Cytological changes accompanying the growth of poliomyelitis virus in cells of human origin (strain HeLa). *Virology*, 1956, 2, 109–125.

28. BEALE, A. J.; STEVENS, P. F.; DAVIS, N.; STACKIW, W., and RHODES, A. J. The development of inclusions in tissue cultures of monkey kidney epithelial cells infected with poliomyelitis virus. *Canad. J. Microbiol.*, 1956, 2, 298–303.

29. NUNEZ-MONTIEL, O.; WEIBEL, J., and VITELLI-FLORES, J. Electron microscopic study of the cytopathology of ECHO virus infection in cultivated cells. *J. Biophys. & Biochem. Cytol*, 1961, 11, 457–468.

30. HOWES, D. W., and MELNICK, J. L. The growth cycle of poliovirus in monkey kidney cells. I. Maturation and release of virus in monolayer cultures. *Virology*, 1957, 4, 97–108.

31. KALLMAN, F.; WILLIAMS, R. C.; DULBECCO, R., and VOGT, M. Fine structure of changes produced in cultured cells sampled at specified intervals during a single growth cycle of polio virus. *J. Biophys. & Biochem. Cytol.*, 1958, 4, 301–308.

The expert assistance of Mr. Bill M. Boland, Miss Millicent Henry and Mr. John Plowman and the contribution of Mr. Charles Parsons are gratefully acknowledged.

LEGENDS FOR FIGURES

FIG. 1. Normal monkey kidney (MK) cell in a monolayer. The filamentous mitochondria of the endoplasm, some of which closely invest the nucleus, sparse lipid globules, and the contiguity of adjacent cell membranes (arrow) are demonstrated in these flattened cells. Living, phase contrast. × 440.

FIG. 2. Two MK cells showing changes typical of early stage of infection 4 to 4½ hours after inoculation of ECHO-9 virus, 10^6 TCID. The cells have retracted from their neighbors. The nuclear outlines are less distinct as a result of accumulation of phase-dense material about them. The nucleoli are somewhat condensed. The mitochondria, especially those near the cell centers, have become shorter and nodose. More lipid granules are evident. Living, phase contrast. × 440.

FIG. 3. An MK cell 4½ hours after inoculation of ECHO-9 virus (10^6 TCID). Phase-dense material is present on the nucleus, which is no longer spherical. There are loose perinuclear accumulations of lipid granules. A few discrete dense bodies (ra) are present in the cell cortex at the surface, and large vacuoles (vac) are present in the endoplasm. This is the first frame of a sequence studied by Mr. Charles Parsons. All are living, phase contrast. × 400.

FIG. 4. Same cell at 5¾ hours. The nucleus has collapsed and its outline is irregular and indented. Lipid granules are now tightly concentrated around the nucleus. Many dense bodies (ra), the basophilic masses seen in stained preparations, are now apparent in the cortex near the hyperactive cell surface in the course of extrusion. Many vacuoles are now evident in the cell; those shown at "vac" are migrating to the periphery. Some have burst to the exterior (arrow).

FIG. 5. Same cell at 6¼ hours. Further retraction of the cell body leaves long peripheral processes. Extrusion of the bodies at the cell periphery and formation of short processes results from bursting (arrow) of underlying vacuoles (vac) at the surface. Many processes contain residual phase-dense bodies, of the kind labeled "ra."

FIG. 6. Same cell at 6 hours, 25 minutes. Continued retraction and nuclear shrinkage. A group of large vacuoles (vac) at the surface, separated by narrow bands of cytoplasm, are in course of bursting.

FIG. 7. Same cell at 6½ hours, markedly retracted. The vacuoles have opened to the exterior. Remaining dense bodies (vac) are adherent to the intervening cytoplasm. The dendritic appearance of the cell results from peripheral vacuolar fusion and their opening to the exterior.

FIG. 8. Same cell at 7 hours. Continued retraction, vacuolation and attenuation of processes. Release of the bodies (basophilic masses) is almost complete.

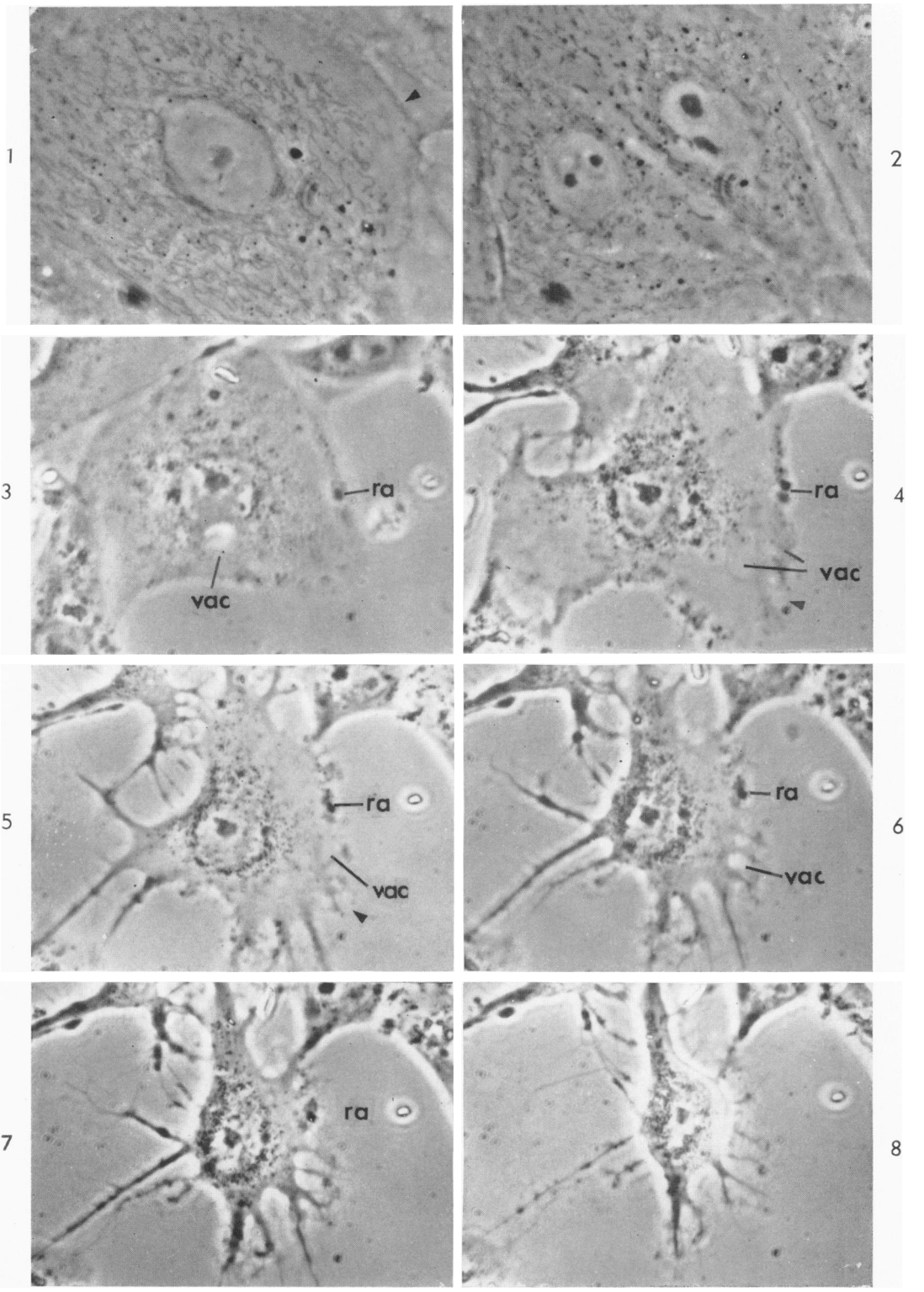
1
2
3
ra
vac
4
ra
vac
5
ra
vac
6
ra
vac
7
ra
8

FIG. 9. Cell in an intermediate stage of infection. Shown are the shrunken and convoluted nucleus (N), its condensed nucleolus and chromatin, the juxtanuclear concentration of vesicles (C) and the surrounding wreath of dense mitochondria (m). Large lipid bodies (l) and some viral crystals (V) are evident. The dilated perinuclear space with its invaginations is well shown (arrow). × 9,240.

FIG. 10. Cell in an intermediate stage of infection after supravital administration of neutral red (dense black globules) which continues to be concentrated in the juxtanuclear central mass. The eccentric nucleus (N) and mitochondrial wreath (m) are marked. Living, phase. × 1,300.

FIG. 11. Same cell 40 minutes later. Extreme vacuolation of the endoplasm (vac) and bursting of a peripheral vacuole (arrow) are shown. The membrane of the collapsed nucleus (N) is pulled into parallel ridges upon which are deposits of moderately dense material. Living, phase. × 1,900.

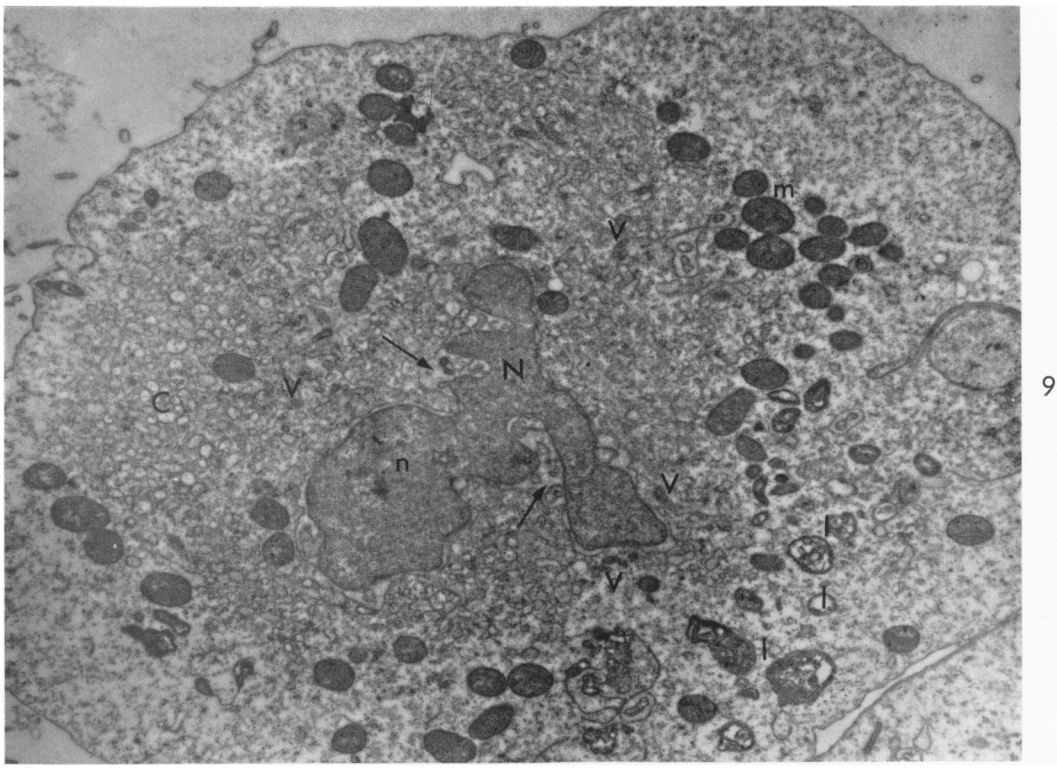

9

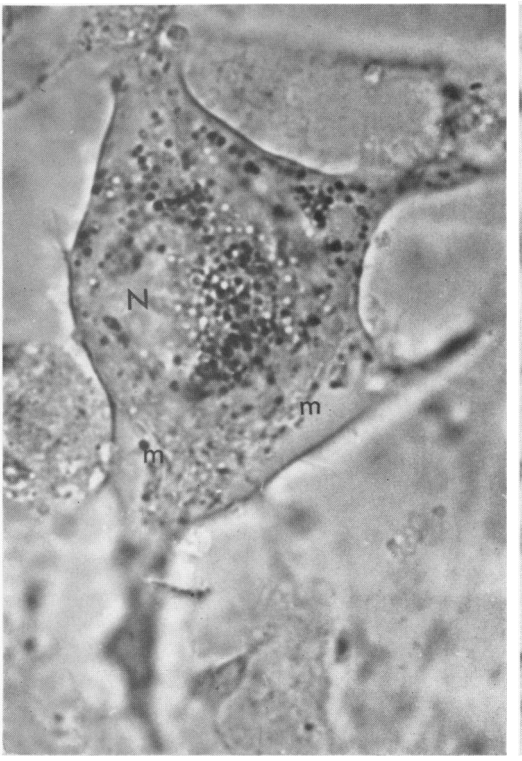

10

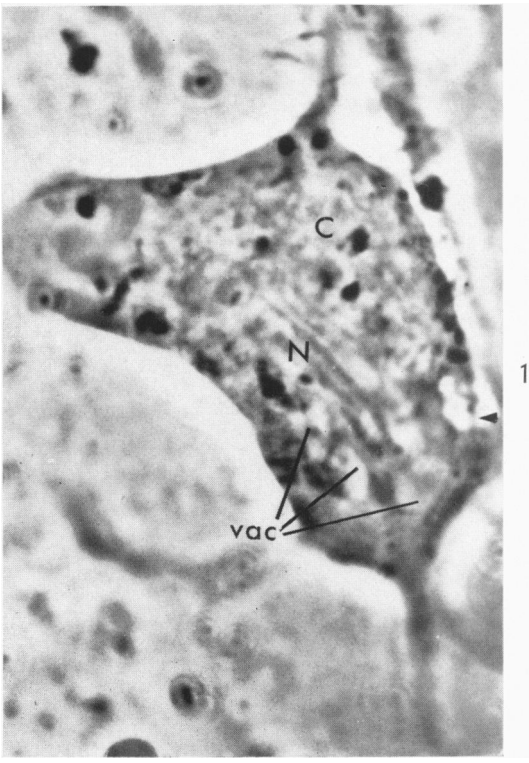

11

FIG. 12. A segment of an MK cell in intermediate stage of infection. Part of the collapsed and wrinkled nucleus (N) is shown; its ridges are packed with condensed chromatin. In the infoldings between them, outside the nuclear membrane, lie aggregates of ribosomes (ra). Looser ribosomal aggregates are shown at the cell periphery (ra′). A dilated part of the perinuclear space appears at the arrow. Nucleolus, n. Mitochondria of the wreath surrounding the juxtanuclear mass, m. The congeries of vesicles making up the juxtanuclear mass occupy the whole cell center. Viral crystals, V; myelin-like lipid bodies, l. × 23,500.

Inset. Detail showing that the ribosomal aggregates are composed of serpentine or linear clusters (files) of ribosomes. × 38,000.

FIG. 13. Whole mount of a cell in a stage of infection comparable to that shown in Figure 19. Details in the collapsed and wrinkled nucleus are not well demonstrated. The peripheral basophilic masses, which are the ribosomal aggregates, are well shown. The mitochondria (m) with apparently enhanced basophilia stand out against the chromophobic central (juxtanuclear) mass. Freezing-substitution, azure B stain. × 2,000.

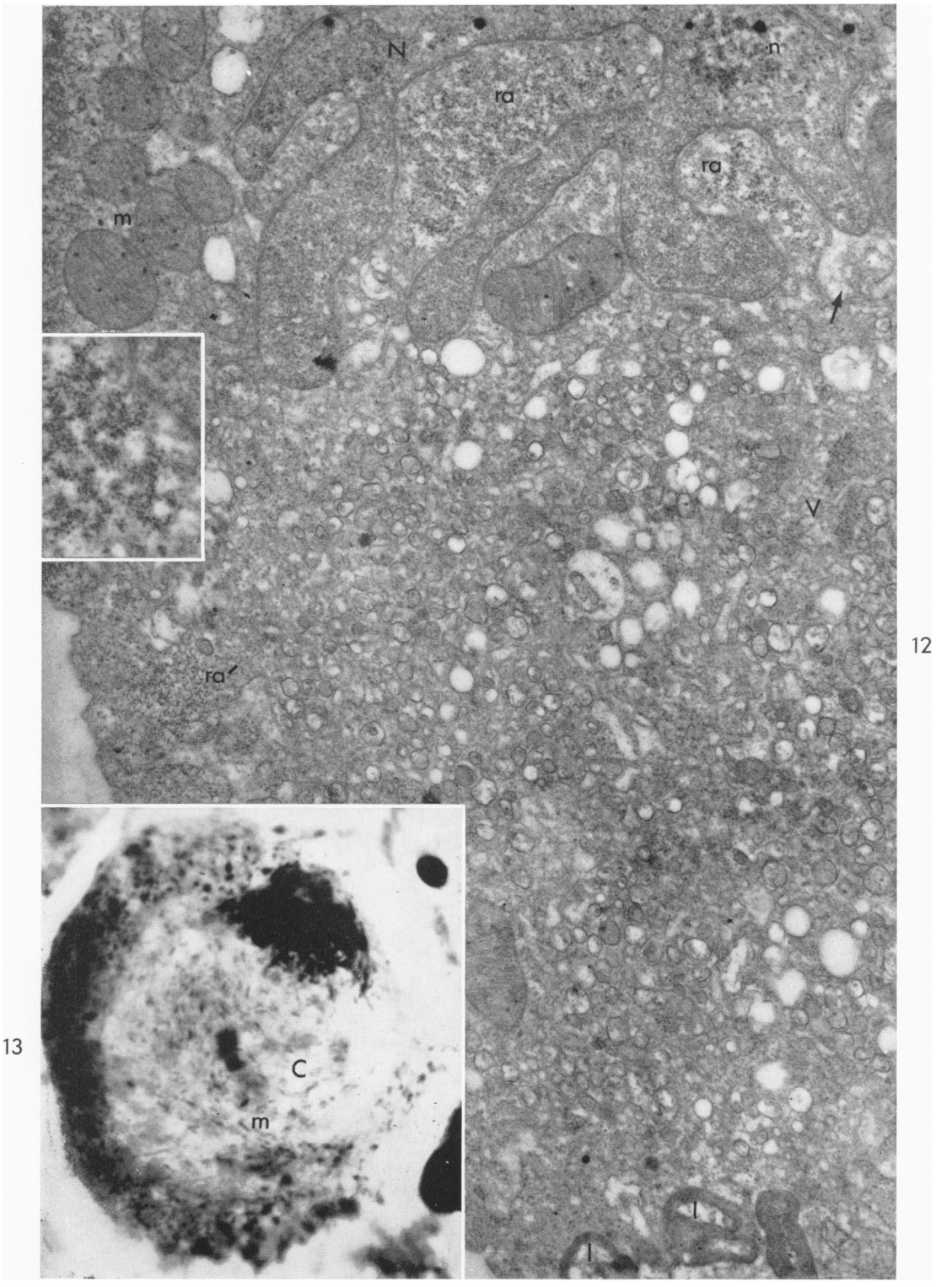

12

13

FIG. 14. Infected cell in process of shedding pieces of its cortical cytoplasm by detachment of tabs, some of which contain ribosomal aggregates (ra). Cortical ribosomal aggregates within the cell, ra′. Virus (V) is also shed at the cell surface. × 10,000.
Inset. Detail of a pedunculated tab or protrusion containing ribosomal aggregates. After detachment, the peduncle or process adherent to the cell is retracted in the form of a scroll. × 42,000.

FIG. 15. Whole mount of an infected cell showing the extent of shedding of tabs of cortical cytoplasm. Numerous vacuoles are present in the cell. Freezing substitution, azure-eosin stain. × 1,000.

FIG. 16. Ribonucleoprotein masses (ra) at the periphery in process of being shed. Freezing substitution, azure B stain, yellow-green filter. × 1,200.

FIG. 17. ECHO-9 antigen in ribosomal aggregates being shed at cell surface. Compare with Figure 23. Indirect fluorescent antibody technique. × 800.

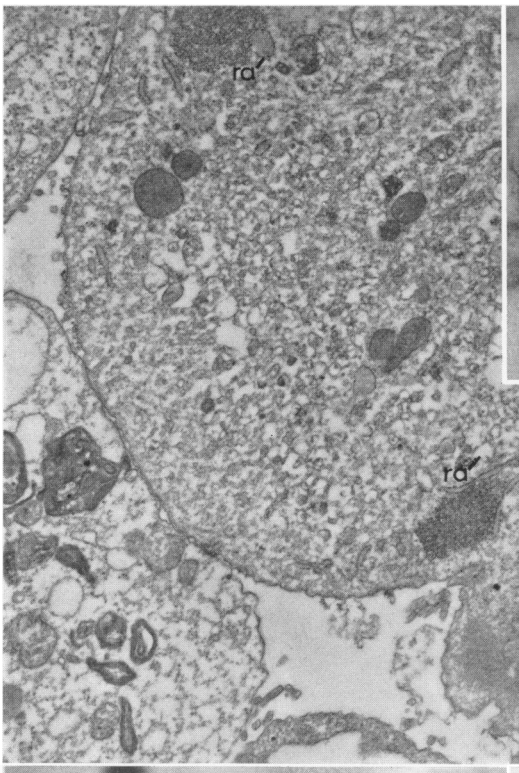

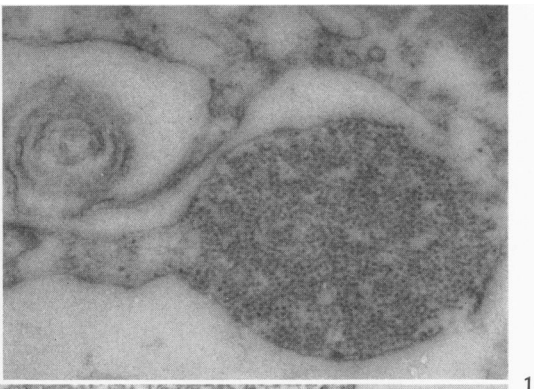

14

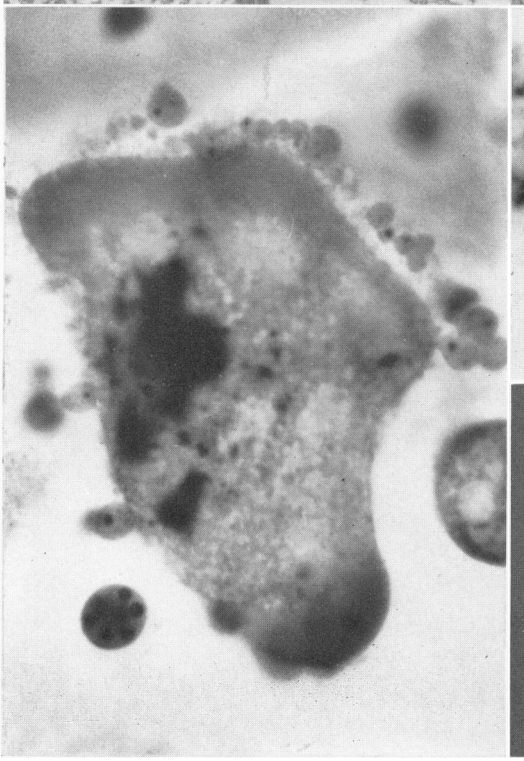

15

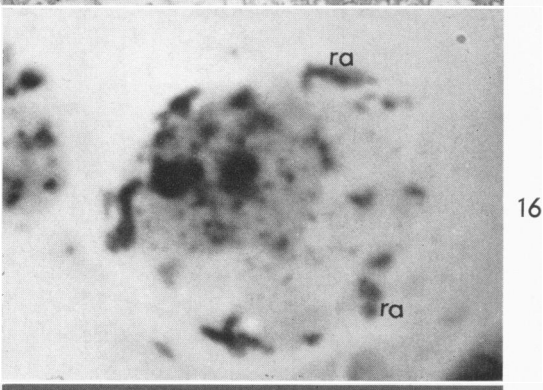

16

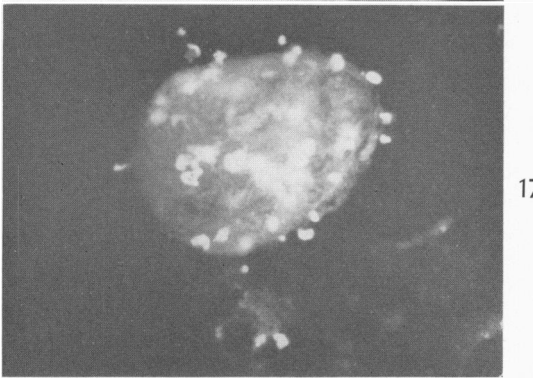

17

FIG. 18. An infected cell contains large vacuoles (vac) which develop by dilatation of smooth-walled vesicles and remnants of endoplasmic reticulum (er) and subsequent fusion. Diffuse, moderately dense material is present in the largest vacuoles. Myelin-like lipid bodies, l. × 10,000.

FIG. 19. Large peripheral vacuole (vac) in the act of bursting at the cell surface and lifting off an overlying sheet of cytoplasm containing some phase-dense masses (ribonucleoprotein, ra). It will become a short process and subsequently be detached. The mantle of phase-dense material in the cortex represents the ribonucleoprotein. Living, phase contrast. × 1,500.

FIG. 20. Infected cell whose cortex has been extensively infiltrated by vacuoles retained by a spongework of intervening lamellas and bridges of cytoplasm. The juxtanuclear zone is stained solidly black. Sudan black B stain. × 400.

FIG. 21. Infected cell stained to show distribution of acidophilic protein. Vacuolar contents are unstained; nucleus (N) is relatively poorly colored but ribonucleoprotein-containing mantle zone has greatest concentration. Frozen-substituted, fast green FCF stain at pH 2.4. × 1,200.

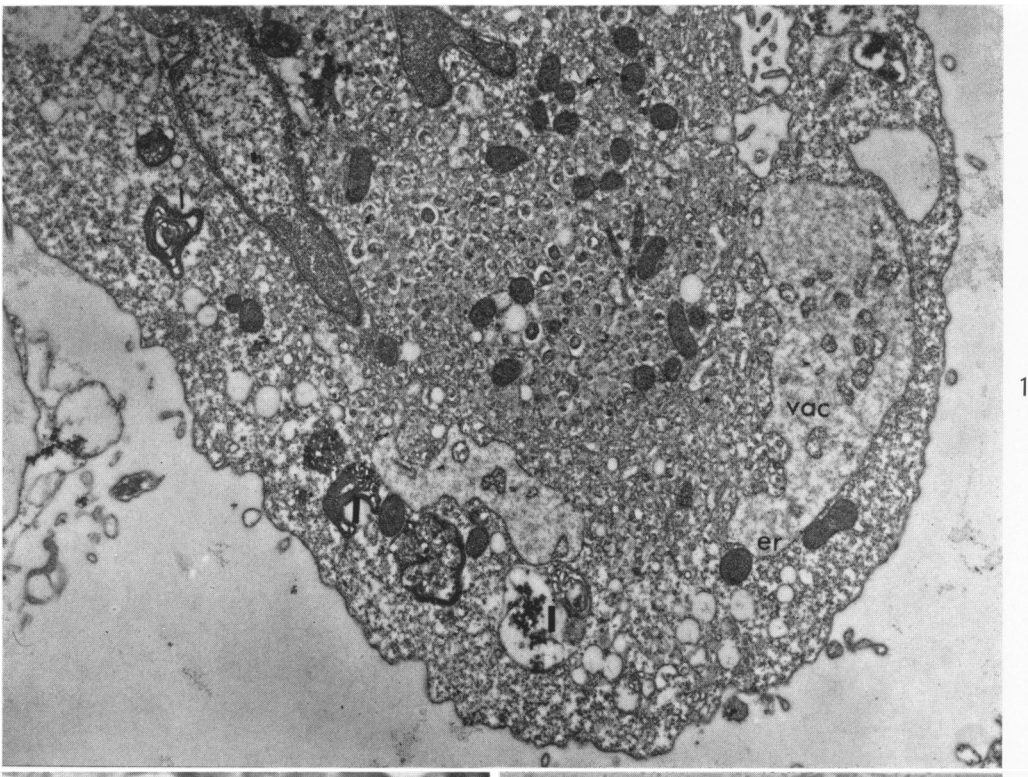

18

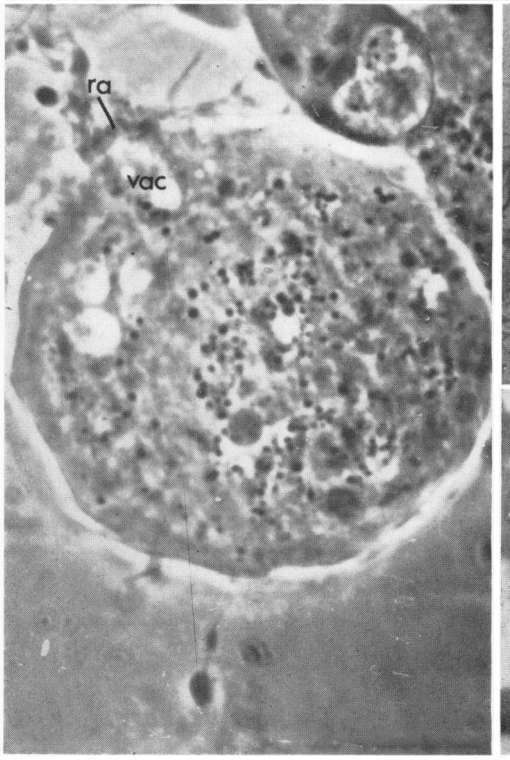

19

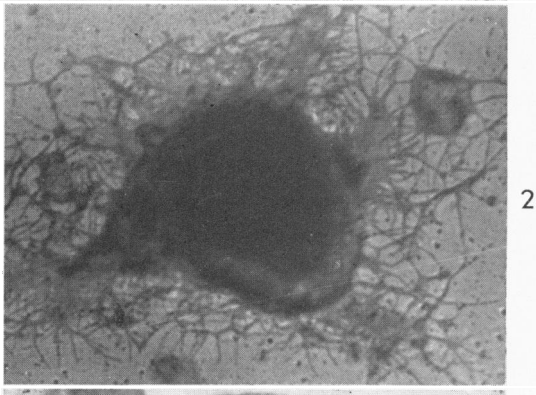

20

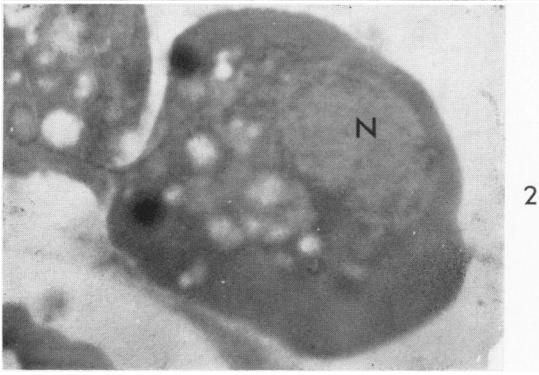

21

FIG. 22. An altered nucleus (N) early in the mid phase of infection. There is margination of the condensed chromatin which fills the gyri or outpocketings; it has a finely filamentous appearance. The somewhat disorganized nucleolus, in which the nucleolonemata are poorly defined, N; a fenestra is present at f and a viral crystal at V. Paracrystalline intranuclear bodies of unknown nature, b. × 18,000.

FIG. 23. The nucleus in a more advanced stage of condensation and shrinkage. The finely filamentous character of the more compacted chromatin is better shown. The disarrayed remnant of nucleolus is shown at n, and 3 bodies of unknown kind are seen at b, of which b′ exhibits crystalline order. The perinuclear space is widened. Viral crystal, V; myelin-like lipid bodies, l. Small dense intercristal particles appear in the mitochondria, m. × 23,000.

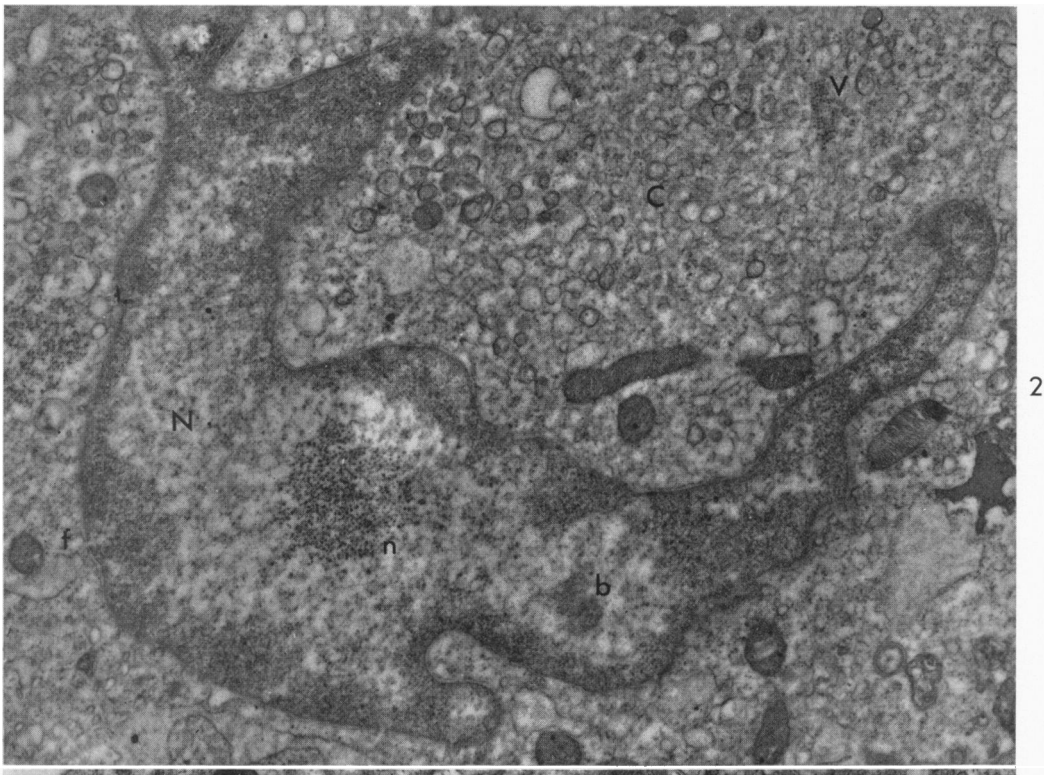

22

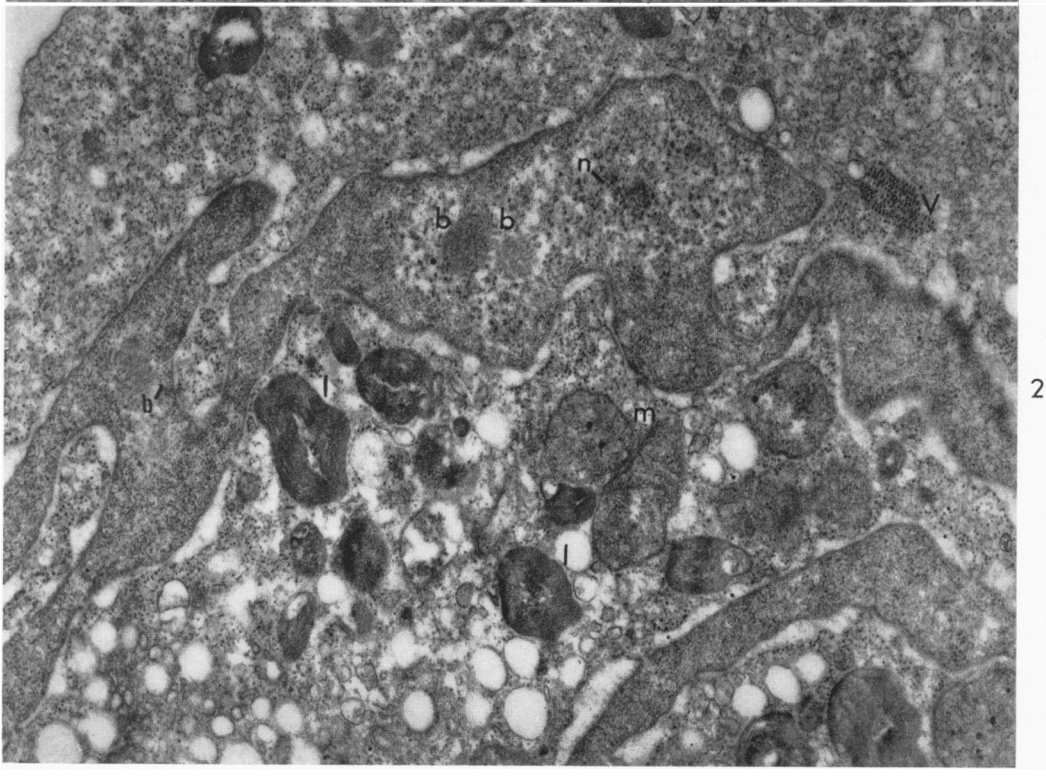

23